Virtual Flow Meter for Chilled Water Loops in Existing Buildings

Eric Mcdonald[1], Radu Zmeureanu[1] and Daniel Giguère[2]
[1]Centre for Zero Energy Building Studies, Department of Building, Civil and Environmental Engineering, Concordia University, Montreal, Quebec, Canada
[2]CanmetENERGY Natural Resources Canada, Varennes, Quebec, Canada

ABSTRACT

This paper presents the application of a Virtual Flow Meter (VFM) with two case studies of central cooling plants in existing buildings. In the first case study, the VFM is used under five different scenarios of available number of sensors, installed on the cooling system, to compare the models predictions when the number of sensors is reduced from eight to four to estimate the chilled water flow rate. In the second case study, the VFM is used with four sensors installed on the cooling system. The estimates of chilled water flow rates are compared with measurements of 10-min time step (first case study) and 15-min time step (second case study). The results from the uncertainty analysis are also presented. The predicted chilled water flow rates agree with the measured values with a coefficient of variance of the root mean squared error (CV(RMSE)) of 5.4-57.5% in the first case study, and 13.5-20.1% in the second one.

1 Introduction

The idea of virtual sensors, or soft sensors, is used in many different industries such as the automotive, the pulp and paper, and is becoming very popular in the heating ventilation and air-conditioning (HVAC) indrustry. A virtual sensor estimates or simulates "measurements" at positions in a system where a physical sensor does not exist, using a mathematical model along with some available measurements from the system.

It is expensive to install sensors in all points of interest in a HVAC system and all zones in a building, and then connect them with a building automation system (BAS). For this, Tahmasebi et al. (2013) created virtual sensors or virtual data points to reduce the amount of sensors that are required for the calibration of building energy models. Zach et al. (2013) developed an approach to implement simulation-powered virtual sensors in a building information framework. Two prototypical virtual sensors were introduced to demonstrate the methodology of the proposed framework. The virtual sensors estimate radiator heat power and the visual conditions at any location.

Virtual sensors have been used to estimate the chilled, condenser and hot water mass flow rates in the HVAC system. They are used at the (1) pump station (Song et al. 2012, Wang et al. 2010); (2) air handling unit (AHU) (Swamy et al. 2012); and (3) chiller (Zhao et al. 2012).

Wang et al. (2012) determined that the water flow rate after the pump can be estimated by using two measured inputs; the pump head (H), measured with a differential pressure sensor across the pump, and the electric power input (W_{motor}) along with the manufacturer pump curve.

Song et al. (2012) determined that the water flow rate could be estimated by two measurable inputs; the pump speed (ω) and the pump head (H), and using pump performance data. The pump speed is determined by the percentage value of the variable speed drive (VSD) installed on the pump. This is based on the assumption that the VSD is calibrated to the correct speed of the pump. A differential pressure transducer determines the pump head across the pump. The challenges associated with this model were the calibration of the VSD to the actual pump speed and the creation on an empirically determined in-situ pump curve. The creation on an empirically determined in-situ pump curve requires the use of an ultrasonic flow meter to measure the water flow rates at different levels of pump head to acquire the in-situ pump curve at full speed. The in-situ pump curve is required to be re-calibrated over the lifetime of the pump to continuously acquire accurate results.

Swamy et al. (2012) used one control valve in series with the cooling or heating coil and measured the pressure drop across each component. The differential pressure across the coil (ΔP_C), the valve (ΔP_V) and the total pressure (ΔP_L) across the loop of the system along with the valve authority (N) are used to estimate the water flow rate.

Zhao et al. (2012) used the measurements from sensors installed in a centrifugal chiller to estimate the chilled and condenser water mass flow rate. The method uses a steady-state thermodynamic analysis of the chillers' vapor compression cycle. The developed model was used in the development of decoupling features for fault detection and diagnostics (FDD) of a centrifugal chiller to predict multiple simultaneous faults (Zhao et al. 2011). The methodology by Zhao et al. (2012) estimates the chilled and condenser water mass flow rate and requires ten sensors to be available within the HVAC system. In existing buildings, this complete set of measurements is not always available and it can be difficult and expensive to add permanently installed sensors to the system for the missing measurements.

A new methodology was developed to estimate the chilled and condenser water mass flow rate under different scenarios of available sensors for reciprocating and centrifugal chillers installed in a cooling system, to reduce the number of sensors required from ten to six (McDonald and Zmeureanu 2014). In section 2 the methodology is presented briefly, and in section 3 and 4 the results are presented for two case studies of two buildings in operation with a reciprocating chiller (section 3) and a centrifugal chiller (section 4) installed in the cooling system.

2 Proposed Virtual Flow Meter (VFM) Model

The proposed VFM package uses two different approaches of a steady-state thermodynamic component model of the vapour-compression cycle of a chiller to determine the chilled water flow rate for different scenarios of available sensors installed in the system. The first approach is based on the work of Zhao et al. (2012), which first determines the refrigerant mass flow rate (m_r) by evaluating the thermodynamic energy balance on the compressor (Equation 1) to be used in Equation 2 to estimate the chilled water flow rate of the system. This approach can be applied to any system regardless of the type of the chiller that is installed for scenario 1, 2 and 3.

$$m_r = \frac{W}{(h_{dis} - h_{suc})} \tag{1}$$

where W is the compressor power input, h_{dis} is the discharge enthalpy, which is evaluated from the discharge temperature at the exit of the compressor and the pressure in the

condenser, and h_{suc} is the suction enthalpy, which is evaluated from the suction temperature before the compressor and the pressure in the evaporator.

The second approach integrates some modified subroutines from the ASHRAE HVAC Toolkit of primary systems (Bourdouxhe et al. 1994) to determine the compressor identification parameters for the chiller(s), installed in the cooling system, to be used to determine the refrigerant mass flow rate of the chillers vapour compression cycle. The refrigerant mass flow rate is then used to determine the chilled water mass flow rate (Equation 2). The mathematical models for the VFM are presented in (McDonald and Zmeureanu 2014). Because of space limitations, only the applications of the proposed VFMs are presented in this paper.

The proposed models are analyzed under different scenarios, where each scenario refers to a number of available sensors. Table 1 shows the different scenarios and the required inputs, from sensors, for each scenario. As the amount of available sensors is reduced from scenario #1 (with 10 sensors) to scenario #3 (with 7 sensors) the method uses manufacturer data to estimate the missing information. When the discharge temperature cannot be estimated (scenario #4), a different approach is required to estimate the chilled water mass flow rate. This is achieved by using the subroutines from the primary HVAC toolkit (Bourdouxhe et al. 1994) to provide missing information.

Table 1: List of required sensors or data for each scenario

		Scenario				
Description of point	Symbol	1	2	3	4	5
Manufacturer Data	-	-	-	-	MD-1	MD-1
Condenser water return temperature	T_{cdr}	M	M	M	M	M
Condenser water supply temperature	T_{cds}	M	M	M	M	M
Chilled water return temperature	T_{chwr}	M	M	M	M	M
Chilled water supply temperature	T_{chws}	M	M	M	M	M
Pressure in evaporator	$P_{ref,ev}$	M	M	M	M	M
Pressure in condenser	$P_{ref,cd}$	M	M	M	M	M
Suction temperature	T_{suc}	M	M	E	M	E
Discharge temperature	T_{dis}	M	MD-2	MD-2	-	-
Liquid line temperature	T_{ll}	M	M	E	M	E
Power input into the compressor	W_{ac}	M	M	M	-	-

MD-1 in Table 1 is the manufacturer data used to estimate the refrigerant mass flow rate of the vapor compression cycle for scenarios # 4 and # 5. MD-2 is the manufacturer data used to estimate the discharge temperature (T_{dis}), which is the temperature at the exit of the compressor. M is a measurement, E is a calculated value and (-) denotes the input is not required as inputs to the model.

Equation 2 is used to estimate the chilled water mass flow rate (m_{chw}) and is evaluated under the five different scenarios. For the first three scenarios, the refrigerant mass flow rate (m_r) is calculated from measurements and/or manufacturer's data; for scenarios # 4 and # 5, the HVAC Toolkit is used to estimate the refrigerant mass flow rate.

$$m_{chw} = \frac{m_r(h_{suc} - h_{ll})}{C_p(T_{chwr} - T_{chws})} \tag{2}$$

where h_{suc} is the suction enthalpy, which is determined from the suction temperature and the pressure in the evaporator and h_{ll} is the liquid line enthalpy, which is determined from

the liquid line temperature and the pressure in the condenser. C_p is the specific heat for the chilled water, T_{chwr} is the chilled water return temperature entering the evaporator and T_{chws} is the chilled water supply temperature leaving the evaporator.

The VFM calculates the refrigerants' thermodynamic and transport properties by using REFPROP (Lemmon et al. 2013), a software developed by the National Institute of Standards and Technology (NIST), which is a reference database for fluid thermodynamic and transport properties of pure fluid and mixtures currently available. REFPROP uses published models to calculate the fluids' thermodynamic and transport properties.

3 Case Study # 1 with Reciprocating Compressors

This case study uses measurements obtained from the air-conditioning system of a research laboratory building located in Varennes, Quebec, taken in the of summer of 2012. This case study examined the ability of the VFM to estimate the chilled water flow rate for a reciprocating chiller, for all five scenarios, on a ten-minute time scale that is suitable towards ongoing commissioning analysis of the system.

Overview of Cooling Plant

The refrigeration system consist of a reciprocating chiller operating with refrigerant R-22 that provides chilled water to the air handling unit (AHU) and to two ice storage tanks. The chiller contains two refrigerant lines, which share one common condenser and one common evaporator as shown in Figure 1. The system contains two reciprocating compressors, with the rated capacity of 211 kW (60 tons of refrigeration) each, that can operate with three stages: 33% (with 2-pistons), 66% (with 4-pistons), and 100% (with 6-pistons). The "chilled water" is an ethylene glycol solution of 25% in weight that circulates to the AHU and to the two ice storage tanks.

Control system

The control system was designed to minimize the amount of energy used by the compressor during peak demand periods. The control system has two main modes: (I) ice creation and (II) air-conditioning.

During the ice creation mode, compressor #1 or #2 operate at 100% capacity, valve #1 is closed, and valve #2 is 100% open, so that the chilled water only flows to the two ice storage tanks. The ice creation mode lasts for eight hours or until the ice tanks have reached 100% of their capacity.

In the air-conditioning mode there are two sub-modes: (a) peak usage, and (b) off peak usage. During these sub-modes there are three sequences of operation: (1) with compressor #1; (2) with compressor # 2; and (3) with ice storage tanks. During the peak usage when the electric demand from air-conditioning is high, the system operates with sequences (3-1-2), where the valve #2 is opened to maintain the chilled water supply set–point temperature between 3.2°C and 5.5^{o}C. The compressor #1 is switched on when the ice storage is unable to maintain the set-point temperature; the compressor #2 is switched on only if needed. During the off peak period the system runs with sequences (1-3-2) to maintain the chilled water set point.

To analyze the data for this case study the measurements were separated into the two modes of operation: (1) ice creation and (2) air-conditioning. The ice creation mode is

dominated by steady-state operation of the chillers, while the air-conditioning mode contains fewer durations of steady-state operation.

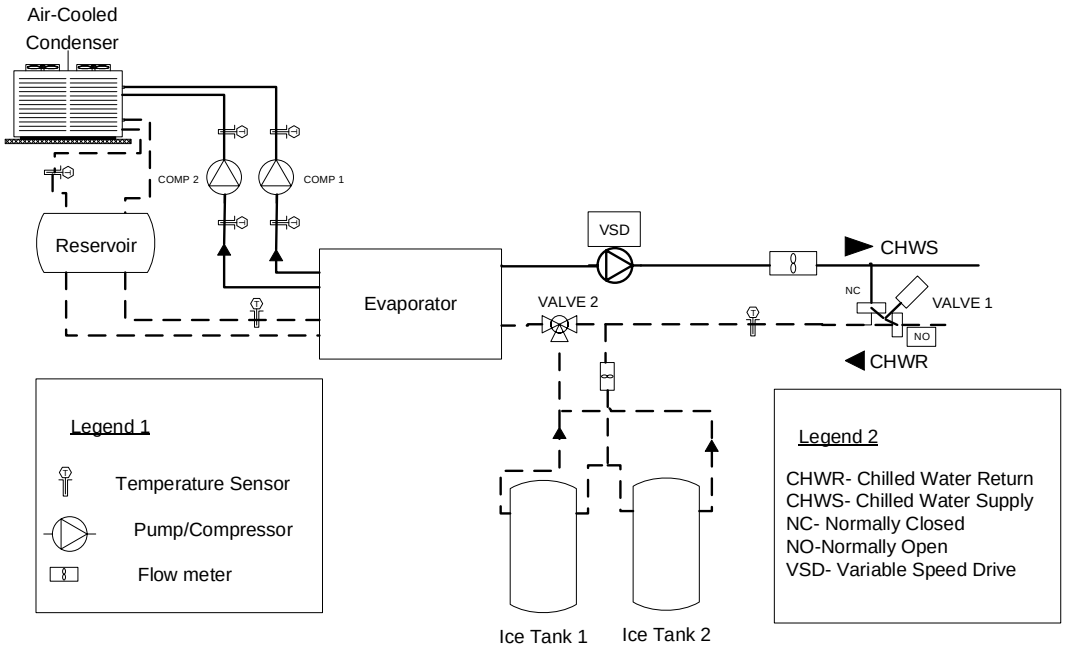

Figure 1: Layout of refrigeration system from CANMET

Instrumentation and available data

The system records measurements for all sensors on a 10-mn time interval (Table 2). Figure 2 shows a simplified diagram of the sensors location on a refrigerant loop.

Table 2: Description of measurements used in case study #1.

Measurement	Variable Name	Instrument	Uncertainty
Temperature	T_{suc}, T_{dis}, T_{ll}	RTD	± 0.1°C
Pressure	$P_{ref,evap}$, $P_{ref,cd}$	Pressure Transducer	± 1% of FS
Flow rate	$\dot{m}_{chw}$	Ultrasonic flow meter	± 0.5 FS

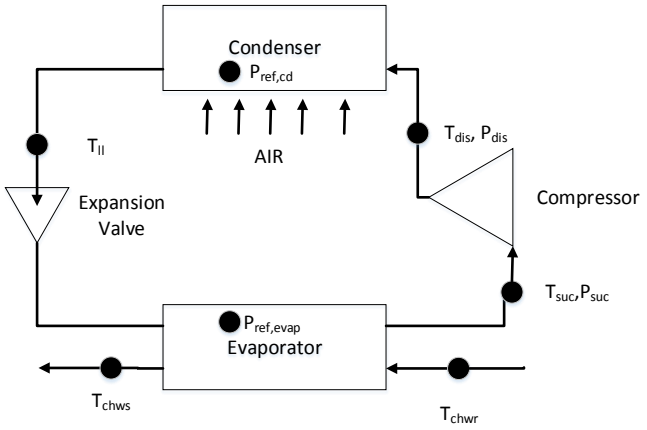

Figure 2: Simplified schematic of refrigeration loop with sensors

Results for Ice creation mode

In the ice creation mode only one compressor is in operation at a time and the pump VSD is set to 65%; the monthly average measured chilled water flow rate is 6.6-6.7 kg/s. Using the proposed method for the VFM, the chilled water mass flow rate was estimated for all five scenarios over four months from June to September, 2012.

Table 3 shows the estimated average refrigerant mass flow of each month for each compressor. The calculated uncertainty associated with the propagation errors from the measurements is also listed. The refrigerant mass flow rates estimated for the two compressors are different because of the difference in the measurements for each compressor. The suction temperature is different between compressors # 1 to 2 with a difference of 20 ^{o}C that causes the differences in scenario 1, 2 and 3. For scenarios # 4 and 5, the main effect comes from the difference between the measured evaporative pressure, which is 273 kPa for compressor # 1, and 378 kPa for compressor # 2. This difference in pressure results in a 10 ^{o}C difference between the saturation suction temperatures (SST) of both compressors, which causes differences in the refrigerant mass flow rate from 0.39 kg/s to 0.64 kg/s.

The calculated refrigerant mass flow rate is then used to estimate the chilled water mass flow rate (Equation 2). Table 4 shows the predicted chilled water flow rate for both compressors over each month of the observed period. The VFM results for compressor # 1 compare well with the monthly average measured chilled water flow rates over all five scenarios. The results of scenario # 5 has the lowest coefficient of variance of the root mean squared error (CV(RMSE)) of 5.4% (Table 5), followed by scenario # 3 (15.6%) and # 1 (22.8%). The differences from one scenario to another comes from the differences in the both the refrigerant mass flow rate and in the liquid line enthalpy (hll) (Table 6). Scenario # 4 seemed unable to provide a good estimate of the chilled water mass flow rate as it deviated by 2.3 kg/s and a CV(RMSE) of 53.4%.

Table 3: Comparison of estimated refrigerant mass flow rates (kg/s) for compressor # 1 and # 2

Scenario	Compressor	June	July	August	September
1	Comp #1	0.72 ±0.04	0.84 ±0.01	0.85 ±0.04	0.95 ±0.02
	Comp #2	0.51 ±0.01	1.01 ±0.06	0.68 ±0.03	0.49 ±0.08
2	Comp #1	0.38 ±0.02	0.40 ±0.01	0.40 ±0.01	0.37 ±0.03
	Comp #2	0.54 ±0.01	0.51 ±0.04	0.52 ±0.03	0.56 ±0.01
3	Comp #1	0.47 ±0.02	0.50 ±0.01	0.49 ±0.01	0.46 ±0.04
	Comp #2	0.60 ±0.01	0.58 ±0.04	0.59 ±0.03	0.53 ±0.01
4	Comp #1	0.37 ±0.04	0.38 ±0.05	0.38 ±0.06	0.36 ±0.07
	Comp #2	0.65 ±0.07	0.61 ±0.07	0.62 ±0.04	0.64 ±0.01
5	Comp #1	0.41 ±0.04	0.42 ±0.05	0.42 ±0.04	0.40 ±0.08
	Comp #2	0.68 ±0.07	0.65 ±0.07	0.66 ±0.04	0.62 ±0.05

In the case of compressor # 2, the same method was followed as for compressor # 1 but the VFM model was unable to estimate the chilled water flow rate within the same confidence for each scenario as for compressor # 1. Scenario # 2 and 4 gave the best results with a CV(RMSE) of 16.7% and 28.9%, respectively. The main difference between the two compressors comes from the differences in the pressure in the evaporator and the suction temperature (T_{suc}). These two inputs have different effects on the predictions of each scenario and cause the differences in the predictions as the estimation of the average chilled water flow rate differs when the model is applied to the different compressors.

For compressor # 1, under scenarios # 1, 3 and 5 the predicted average chilled water flow rates over the summer season are 5.6 kg/s, 7.8 kg/s and 6.6 kg/s that compares well with the measured value of 6.7 kg/s under the given uncertainties. For compressor # 2, under scenario # 2, and # 4 the predicted average chilled water flow rates over the summer season are 5.8 kg/s and 5.2 kg/s that compares well with the measured value of 6.7 kg/s under the given uncertainties. The uncertainties due to the propagation of the measurement error for each scenario are given in Table 4a and 4b. The uncertainties were determined by applying the taylor series method for cross-sectional data as described by Reddy (2011) to Equation 1 and 2, which was evaluated it for each scenario. Because of space limitations, only the results for the uncertainties are presented in this paper.

Table 4a: Compressor # 1 in operation in ice creation mode

Month	hours	$\dot{m}_{chw}$ (kg s^{-1})					
		Measured ± 1.2	1	2	3	4	5
June	6	6.7	5.1 ± 0.7	5.3 ± 0.7	7.7 ± 1.0	4.4 ± 0.6	6.7 ± 0.9
July	23	6.7	5.6 ± 0.6	5.5 ± 0.5	8.1 ± 0.8	4.5 ± 0.4	6.9 ± 0.6
August	34	6.6	5.3 ± 0.4	5.2 ± 0.4	7.6 ± 0.6	4.3 ± 0.3	6.5 ± 0.5
September	9	6.7	5.8 ± 0.6	5.1 ± 0.6	7.4 ± 0.8	4.2 ± 0.4	6.3 ± 0.7
Average	-	6.7	5.6 ± 0.6	5.2 ± 0.6	7.8 ± 0.8	4.4 ± 0.4	6.6 ± 0.8

Table 4b: Compressor # 2 in operation in ice creation mode

Month	hours	$\dot{m}_{chw}$ (kg s^{-1})					
		Measured ± 1.2	1	2	3	4	5
June	38	6.7	4.5 ± 0.4	5.9 ± 0.6	9.8 ± 0.8	5.2 ± 0.5	11.0 ± 1.0
July	28	6.7	10.7 ± 1.2	6.0 ± 0.6	10.1 ± 1.0	5.4 ± 0.6	11.3 ± 1.1
August	27	6.6	6.1 ± 0.6	5.7 ± 0.5	9.4 ± 0.8	5.0 ± 0.5	10.5 ± 0.9
September	7	6.6	7.5 ± 0.7	5.4 ± 0.8	8.9 ± 1.3	5.0 ± 0.8	10.5 ± 1.5
Average	-	6.7	7.2 ± 0.6	5.8 ± 0.8	9.6 ± 1.0	5.2 ± 0.6	10.8 ± 0.6

Table 5: CV(RMSE) (%) of both compressors in the ice creation mode

	Scenario				
	1	2	3	4	5
Compressor # 1	22.8	25.6	15.6	53.4	5.4
Compressor # 2	57.5	16.7	33.6	28.9	40.3

Uncertainty of sub-cooling measurements

This case study presented one challenge due to the accuracy of the sensor installed on the liquid refrigerant line (T_{ll}). The observed amount of sub-cooling (ΔT_{ll}) for compressors #1 and 2, determined from measurements, were greater than zero (Figure 3), while the observed amount of sub-cooling presented in the original commissioning of the system was -11.1°C. Hence, it was difficult to assess if the refrigerant completely condenses in the condenser or not. The temperature sensors measured the pipe surface temperature, which can differ from the correct fluid flow temperature. The effect of solar radiation has a large effect on the pipe surface temperature and can cause large variations between the measured temperature and the actual fluid temperature (Gorman et al. 2013). The sensors used for the condensing temperature are located close to the air-cooled condenser on the roof of the building, which can be effected by solar radiation, wind, and rain that can cause the sensor measurement to be different from the real fluid temperature.

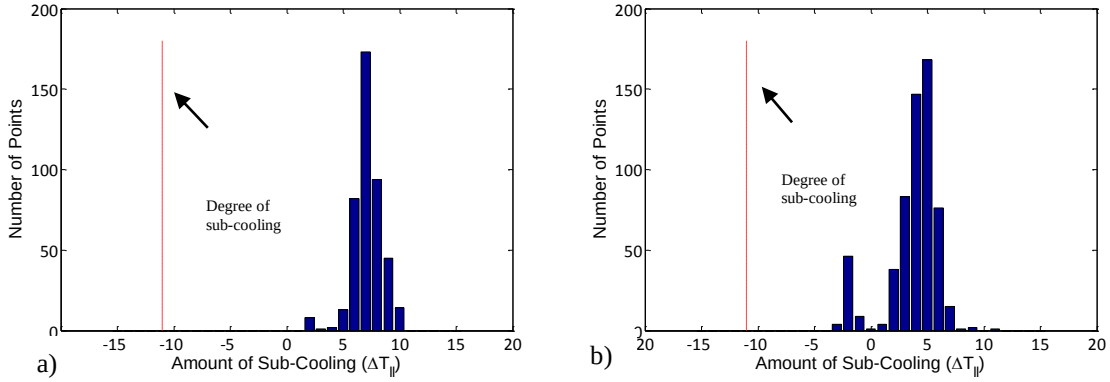

Figure 3: a) Amount of sub-cooling for compressor # 1 from measurements b) Amount of sub-cooling for compressor # 2 from measurements

To solve this particular problem, the measured chilled water flow rate (m^*_{chw}) is used to determine the energy balance on the evaporator (Equation 3) was used to estimate the liquid line enthalpy (h^*_{ll}), from the chilled water side. Table 6 shows the calculated average enthalpy (h^*_{ll}) for each scenario #1, #2 and #4, which uses the measured liquid line temperature (T_{ll}) as an input; and the calculated average quality (X) of the refrigerant leaving the condenser. The quality was determined from the average enthalpy (h^*_{ll}) and the saturation discharge temperature (SDT).

$$h^*_{ll} = h_{suc} - \frac{m^*_{chw} C_p (T_{chwr} - T_{chws})}{m_r} \quad (3)$$

where h_{suc} is the suction enthalpy, which is determined from the measured suction temperature and the measured pressure in the evaporator. C_p is the specific heat for the chilled water which is 3.67 kJ*(kg*k)$^{-1}$ and T_{chwr} is the measured chilled water return temperature entering the evaporator and T_{chws} is the measured chilled water supply temperature leaving the evaporator.

Table 6: Calculated average enthalpy and quality of liquid refrigerant leaving the condenser for ice creation mode

	Scenario					
	1		2		4	
	h_{ll} (kJ/kg)	X (%)	h_{ll} (kJ/kg)	X (%)	h_{ll} (kJ/kg)	X (%)
Compressor # 1	345	58	292	26	316	40
Compressor # 2	319	44	298	32	329	51

These results led to the conclusion that the refrigerant is not fully condensing in the condenser, and in this case, scenarios #1, #2 and #4 cannot be directly used. Hence, we propose for such a case the short-term measurement of the chilled water flow rate, with a portable meter, to help in estimating the leaving refrigerant conditions from the condenser (Equation 2); once this information is available, the proposed VFM could be used for the ongoing estimations. This approach is similar to Song et al. (2012) that used short-term measurements of water flow rate to calibrate the pumps curve. In this case study we used the average quality from Table 6 to evaluate, for continuous measurements the chilled water flow rate under scenarios #1, #2 and #4.

Results for Air-Conditioning Mode

In the air-conditioning mode, the chiller is used with the ice banks to provide chilled water to the AHU. In this mode the compressors can operate at three different loadings to control the capacity delivered to the system. The chilled water pump is also controlled by a variable speed drive (VSD) that allows the flow to change for the different loads required to cool the system during the day. The VFM models are able to predict closely to the measured value. For the compressor #1, the scenarios #1, # 2, and # 4 have the CV(RMSE) value of 27.5%, 15.2%, and 16.9%, respectively (Table 7). For the compressor # 2, the scenarios # 2 and # 4 follow the same trend as for the ice creation mode as have the they estimate the lowest CV(RMSE) value of 17% and 13.1%, respectively.

Table 7: CV(RMSE) (%) of both compressors in the air-conditioning mode

	Scenario				
	1	2	3	4	5
Compressor # 1	27.5	15.2	32.5	16.9	42.0
Compressor # 2	46.5	17.0	33.2	13.1	48.3

Conclusion of Case Study #1

This case study showed that the VFM model is able to predict the chilled water flow rates of a system with a reciprocating compressor within a given uncertainty for five different scenarios of available sensors. A portable ultrasonic flow meter can be used to provide estimation on the average thermodynamic state of the refrigerant during the condensing process to be used to estimate the chilled water flow rate for case studies where the liquid line temperature (T_{ll}) is greater or equal to the SDT. For this case, in absence of a portable ultrasonic flow meter scenario # 3 and # 5 can be used to estimate the chilled water flow rate.

4 Case Study # 2 with a centrifugal compressor

This case study uses measurements obtained from building automation system (BAS) installed in an institutional building over the summer of 2013, which records measurements from the HVAC systems, including the central cooling and heating plant. This case study presents a more common situation in existing HVAC systems, where very few sensors are installed.

Overview of Cooling Plant

The refrigeration system consists of two 3165 kW (900 ton) two-stage centrifugal chillers which are connected in parallel and operate with refrigerant R-123. Two constant speed pumps, connected in parallel, circulate the chilled water from the chillers to buildings. Each pump is turned on according to the number of chillers in operation. The measurement devices for the SST, SDT, the saturation pressure in the evaporator ($P_{ref,evap}$), and the saturation pressure in the condenser ($P_{ref,cd}$) used for this case study (Table 8) are installed inside the chiller and are connected to the BAS. A portable ultrasonic flow meter was used to verify the average chilled water flow rates, which were 86.8 kg/s for a single pump in operation and 144.5 kg/s well both pumps were under operation.

Table 8: Description of measurements used in this case study.

Measurement	Variable Name	Instrument	Uncertainty
Temperature	T_{sat}, T_{sat}	RTD	± 0.25 ^{O}C
Pressure	$P_{ref,evap}$, $P_{ref,cd}$	Pressure Transducer	± 0.3 % FS
Flow rate	$\dot{m}_{chw}$	Portable Ultrasonic	± 2.1 kg/s

Summary of Results

Because of the limited amount sensors available in this system, only scenario # 5 could be used to estimate the chilled water mass flow rate. The chilled water mass flow rate was calculated separately for each chiller in operation as well as when both chillers were in operation; the estimated chilled water flow rates were compared with the measured values. The CV(RMSE) were calculated for each chiller over the complete cooling season from May to September (Table 9). The CV(RMSE) was 20.1% for when chiller # 1 was under operation, 13.6% while chiller # 2 is under operation, and 13.5% while both chillers are under operation. The VFM estimated that the average chilled water flow rate over the complete cooling season was 90.4 ± 19.4 kg/s for chiller # 1 and 85.1 ± 19.4 kg/s for chiller # 2, and 156.2 ± 19.4 kg/s for both chillers under operation which agree well within the uncertainty with the measured result of 86.8 ± 2.1 kg/s for one chiller under operation and 144.5 ± 2.1 kg/s for both chillers under operation.

A steady state filter was developed to filter out the transient conditions caused by the changing conditions inside the chiller. The condensing pressure was determined to be the parameter that has the slowest response to changes in conditions and is used to determine if the system operates at steady state (Zhao et al. 2012). The combination of the slope and standard deviation were monitored over a moving time-window of the condensing pressure to evaluate if the system is in steady state. The uncertainty due to measurements for the VFM is 19.4 kg/s, which is a large amount of uncertainty. The high level of uncertainty comes mostly from the temperature sensors that have a large uncertainty of 0.25^{o}C.

Table 9: CV(RMSE) and MBE for both chillers

	CV(RMSE) (%)	MBE (%)
Chiller # 1	20.1	-15.2
Chiller # 2	13.6	-8.1
Both Chillers	13.5	-11.8

Conclusion of Case Study #2

This case study demonstrated the VFMs' ability to predict the chilled water mass flow rate for a cooling plant consisting of two centrifugal chillers with two constant speed pumps. The average predicted chilled water flow rate agree well with the measured value with a CV(RSME) of 13.5% to 20.1% over the complete cooling season. A steady-state filter was required to automatically filter out the transient conditions to evaluate the VFM model during only steady-state conditions.

5 Conclusions

This paper presented two case studies where a low cost non-intrusive method was used to estimate the chilled water mass flow rate under different scenarios of available sensors. The methodology allows the chilled water mass flow rate to be estimated for reciprocating and centrifugal chillers under different scenarios of available sensors included in the system.

The VFM was able to estimate the chilled water mass flow rate for case study one using different scenarios of available sensors and estimated well the chilled water mass flow rate for 4 scenarios with compressor # 1 with a CV(RMSE) of 5.4-32.5% and for 3 scenarios with compressor # 2 with a CV(RMSE) of 13.1-33.6%. The VFM was able to predicted well the chilled water mass flow rate for the second case study with a CV(RMSE) of 13.5-20.1% for the different modes of operation.

The VFM uses data from sensors available in the systems BAS and the different scenarios allow the model to be integrated without adding additional sensors to the system. This technique can be applied to reciprocating and centrifugal chillers. The estimated chilled water mass flow rate could be used to further monitor the chiller cooling capacity, the chiller efficiency and be used to detect system operation faults with developed fault detection techniques for chillers. In application, the VFM model can be embedded into a BAS to provide a low cost online monitoring tool of the chilled water mass flow rate to be used to continuously monitor the chillers' performance for ongoing commissioning techniques.

6 Acknowledgments

The authors acknowledge the financial support from NSERC Smart Net-Zero Energy Building Strategic Research Network and the Faculty of Engineering and Computer Science of Concordia University and CANMET Energy Technology Centre.

7 References

Bourdouxhe, J. P., Grodent, G. and Lebrun, J. 1994. HVAC toolkit—a toolkit for primary HVAC system energy calculations, Atlanta, GA: American Society of Heating, Refrigerating and Air-conditioning Engineers, Inc.

Gorman, J. M., Sparrow, E. M. & Abraham, J. P. 2013. Differences between measured pipe wall surface temperatures and internal fluid temperatures. *Case Studies in Thermal Engineering,* 1**,** 13-16.

Kim, M., Yoon, S. H., Domanski, P. A. & Vance Payne, W. 2008. Design of a steady-state detector for fault detection and diagnosis of a residential air conditioner. International Journal of Refrigeration, 31, 790-799.

Lemmon, E.W., Huber, M.L., McLinden, M.O. , 2013. NIST Standard Reference Database 23: Reference Fluid Thermodynamic and Transport Properties-REFPROP, Version 9.1, National Institute of Standards and Technology, Standard Reference Data Program, Gaithersburg.

McDonald, E., Zmeureanu, R., (2014) Virtual Flow Meter to Estimate the Water Flow Rates in Chillers. (Accepted for ASHRAE Transactions TRNS-00207-2013).

Reddy, T. A. 2011. Applied Data Analysis and Modeling for Energy Engineers and Scientists, Springer, New York, p 86-89.

Song, L., Joo, I. S., & Wang, G. 2012. Uncertainty analysis of a virtual water flow measurement in building energy consumption monitoring. HVAC and R Research, 18(5), 997-1010.

Swamy, A., Song, L., & Wang, G. 2012. A virtual chilled-water flow meter development at air handling unit level. ASHRAE Transactions, 118(1), 1013-1020.

Tahmasebi, F., & Mahdavi, A. 2013. A two-staged simulation model calibration approach to virtual sensor for building performance data. Building Simulation 2013 Conference, Chambery, France.

Wang, G., Liu, M., & Claridge, D. E. 2010. Development of an energy meter using a pump flow station. ASHRAE Transactions, 116(2), 569-577.

Zach, Z., Hofstatter, H., Glawischnig, S., & Mahdavi, A. 2013. Incorporation of Run-Time Simulation-Powered Virtual Sensors in Building Monitoring Systems. Building Simulation 2013 Conference, Chambery, France.

Zhao, X., Yang, M., & Li, H. 2011. Decoupling features for fault detection and diagnosis on centrifugal chillers (1486-RP). HVAC & R Research, 17(1), 86-106.

Zhao, X., Yang, M., & Li, H. 2012. Development, evaluation, and validation of a robust virtual sensing method for determining water flow rate in chillers. HVAC & R Research, 18(5), 874-889.